



ELSEVIER

Information Sciences 149 (2003) 31–40

INFORMATION
SCIENCES
AN INTERNATIONAL JOURNAL

www.elsevier.com/locate/ins

MEMS tunable gratings with analog actuation

Wei-Chuan Shih *, Chee Wei Wong, Yong Bae Jeon,
Sang-Gook Kim, George Barbastathis

*Department of Mechanical Engineering, Massachusetts Institute of Technology,
77 Massachusetts Avenue, Rm. 3-461c, Cambridge, MA 02139, USA*

Received 27 September 2001; accepted 8 May 2002

Abstract

We have designed and fabricated tunable gratings with period tunable to within fraction of a nanometer. We actuated the gratings by electrostatic and piezoelectric means, and demonstrated period changes of order 1 nm. Fabrication processes for the two versions are presented. Devices characterization and experimental results are given for respective devices.

© 2002 Elsevier Science Inc. All rights reserved.

1. Introduction

Optical microelectromechanical systems (MEMS) is an emerging field in recent years. There are several advantages to scale bulk devices down to micron level. First, because all moving parts have much smaller inertia, MEMS are more sensitive to driving signals, and more immune to environmental disturbances such as random vibration. Second, most designs more or less share the microelectronics processing technology which poses excellent alignment on different parts and drastically reduces the cost.

* Corresponding author.

E-mail address: gbarb@mit.edu (G. Barbastathis).

We here demonstrate a tunable MEMS grating which permits analog control over the diffraction angle, accomplished by analog deformation of the grating structure in the lateral direction. Compared to other tunable grating implementations (e.g. the grating light valve [1] and the polychromator [2]), our device concept trades deflection range for angular resolution. Applications for high resolution analog tunable gratings include microspectrometers, external cavity tunable lasers, and thermal compensators for wavelength multiplexer–demultiplexers. In this paper, we describe two implementations: electrostatic and piezoelectric. Piezoelectric devices are better suited for applications requiring small tuning range and ultra-fine tunability of below 0.1 nm (e.g. one DWDM channel of ~ 40 GHz is equivalent to a few nm period change on the grating). Electrostatics, on the other hand, are appropriate for broader range and coarser tunability.

2. Concepts and design

Analog tunability of our grating devices is achieved by lateral actuation forces on the grating structure, either by electrostatic comb-drives or thin-film piezoelectric actuators, as illustrated in Fig. 1. By contrast, for the digital design, the tuning is achieved by pulling some of the bars downward by electrodes beneath the grating. Intensity modulation is realized by controlling the beam height. The tuning resolution is limited to the beam width ($\sim \mu\text{m}$). Theoretically our devices can have resolution three orders of magnitude better than the digital versions. In the electrostatic device, the grating is comprised of suspended beams supported by flexures. In the piezoelectric device, the grating is etched onto a thin $0.4 \mu\text{m}$ membrane, from which the membrane is deformed to create the desired grating period change.

Fig. 2a illustrates the design schematic of the electrostatic device. Two comb-drive actuators [3] deform the periodic structure. The structure is com-

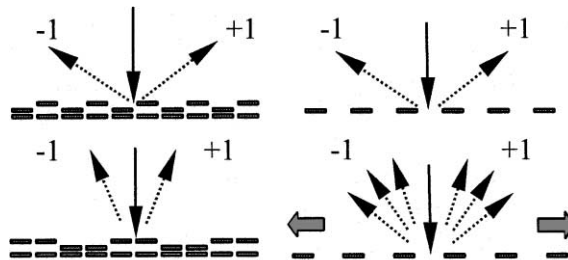


Fig. 1. Actuation concept of an analog tunable grating, permitting analog control of diffraction angle.

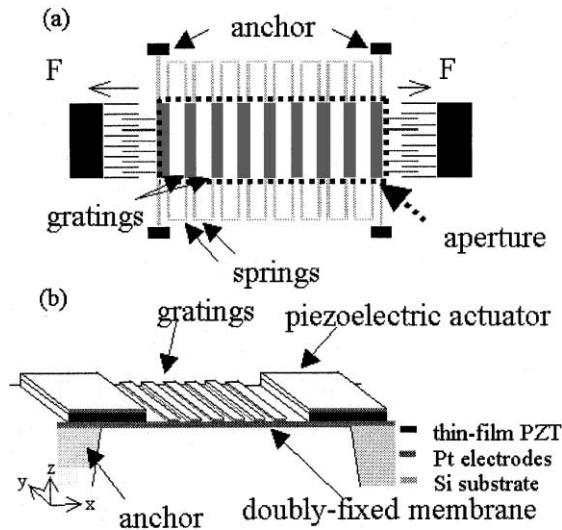


Fig. 2. Design schematic: (a) electrostatic comb-drive actuation and (b) piezoelectric thin-film actuation.

posed of grating bars in the center window and flexures which connect each bar. The flexures determine the stiffness of the entire structure. The suspended structure is attached to the silicon substrate through four anchors.

The stiffness of the flexure can be estimated by $k = Ew^3t/L^3$, where the effective spring constant for one period is on the left side E is the Young's modulus of the material, t is the thickness of the structure, w is the width of the flexure beam, and L is the length of the folded beam. The flexure stiffness is selected based on a trade-off: low tuning voltage (<100 V) requires the device to be compliant. Additionally, we require the device to be stiff enough that the resonant frequency be high. Comb-drive draws essentially no current; therefore, it minimizes power consumption. The disadvantage is that comb-drives deliver small force, usually limited to μN or less. The force can be estimated as $F = -N\epsilon tV^2/2g$, where N is the number of finger pairs, ϵ is the permittivity of air, t is the thickness of the structure, g is the gap distance between two adjacent fingers, and V is the applied voltage. The minimum grating period is set by the resolution of the available lithography tool. Since the flexures on the sides of the grating must be defined, we find the minimum grating pitch is, at best, 4 times the design rule for 75% duty cycle or 6 times the design rule for 50% duty cycle.

In the piezoelectric tunable grating, the driving force is applied via the deposited thin-film PZT (lead zirconate titanate) actuators. The period of the diffraction grating etched onto the membrane is tuned progressively in response

to deflection of the membrane. Fig. 2b illustrates the design in a doubly hinged membrane design configuration.

The in-plane x -deflection δ_x , along the grating period axis, is derived from a piezoelectric bimorph model [4] as

$$\delta_x = \frac{d_{31}E_{\text{pzt}}AV_a}{t_{\text{pzt}}k_x}, \quad (1)$$

where k_x , the effective axial stiffness = $\sum_i E_i A_i / L$, d_{31} the piezoelectric coupling coefficient, E_i the material Young modulus, A_i the cross-sectional area, V_a the applied voltage, t_{pzt} thickness of PZT layer, and L the x -dimension beam length. We note for an isotropic wide beam, $E_i \rightarrow E_i / (1 - \nu_i^2)$ and $d_{31} \rightarrow d_{31} (1 + \nu_i)$, where ν_i the material Poisson's ratio. In our doubly-fixed membrane design (for parameters $d_{31} = -100$ pC/N, $t_{\text{pzt}} = 0.5$ μm , and $L = 450$ μm), this yields a 249 nm x -displacement of the membrane at 10 V actuation and suggests a 3.5 nm grating period change, assuming uniform strain across the membrane. For a 632.8 nm laser on a 4 μm grating period, this corresponds to an angular change of 0.14 mr for the first diffracted order. Given the fine control of piezoelectric actuation against voltage, this provides the resolution of a grating period change well below a nanometer and an angular change below a microradian.

3. Fabrication development

Fig. 3 shows images of the fabricated electrostatic device. A single-mask process is used for the electrostatic grating. Starting with an SOI wafer, lithography followed by DRIE to pattern the grating structure and the comb-drives in the device silicon layer. The buried oxide sacrificial layer is removed

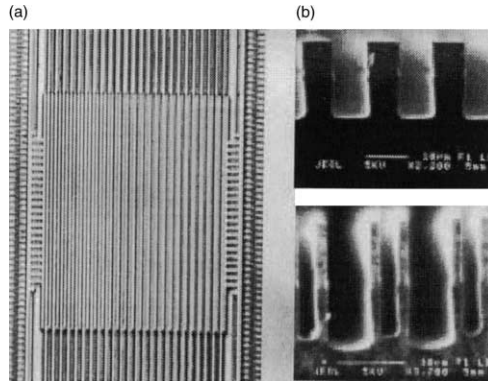


Fig. 3. Tunable electrostatic grating: (a) under optical microscope at 130 \times magnification and (b) SEM of the cross-sections of the gratings (top) and the flexures (bottom).

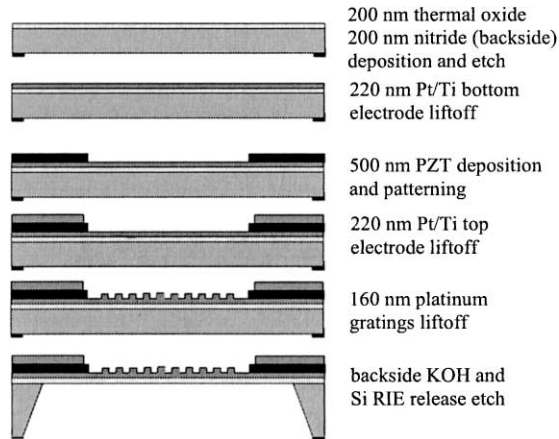


Fig. 4. Piezoelectric device fabrication process flow.

by an HF etching step. Then a maskless metallization step is adopted to coat the reflective surface and bonding pads. Fabrication of the thin-film piezoelectric tunable grating involves both surface and bulk micromachining. Fig. 4 shows fabrication process flow. First, a 200 nm silicon nitride layer is deposited via PECVD and then patterned to form a hard-mask for a later KOH backside etch. A 220 nm Pt/Ti layer is then evaporated on the substrate and patterned via lift-off, creating the bottom electrode. Sol-gel PZT is subsequently spun-on and annealed in several repeated steps to create a PZT layer with 0.5 μm thickness. The piezoelectric layer is patterned via wet-etching [5] and the top electrode deposited with a second 220 nm Pt/Ti evaporation and lift-off procedure. The diffractive grating is next created with a 160 nm Pt lift-off with 2 μm minimal line width features. The doubly-hinged membrane is then defined with a 445 μm KOH backside etch, and finally released with a 5 μm Si RIE.

The fabricated device is shown in Fig. 5. The completed PZT has a predominant perovskite phase aided by good adhesion between the bottom electrode, the SiO_2 diffusion barrier, and the substrate. Ferroelectric characterization suggests an excellent dielectric constant of above 1200, as illustrated in Fig. 6, with an operating frequency range up to 30 kHz. Fatigue lifecycle experiments suggest operation above 10^{10} cycles under a 5 V rectangular pulse-train signal. The fabricated binary phase grating also has duty cycle measured at approximately 66%.

4. Experimental description

We measured the angle change versus actuation voltage with two different methods: optical beam steering with image processing, and the computer

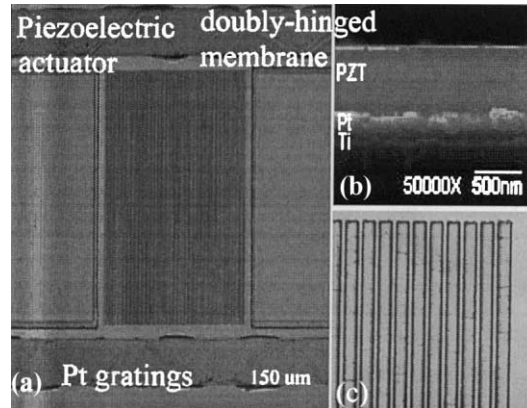


Fig. 5. (a) Piezoelectric-actuated tunable grating under 120 \times magnification, (b) SEM cross-section image of fabricated PZT actuator on Pt/Ti electrodes and (c) magnified view of Pt gratings with 4 μ m period.

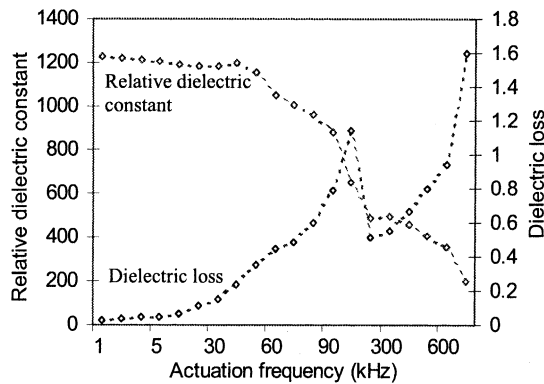


Fig. 6. Ferroelectric characterization of fabricated PZT, with dielectric constant of 1200 below 30 kHz.

microvision technique [6], which involves obtaining three-dimensional images of microscopic targets using the optical sectioning property of a light microscope and post-processing the combined images to analyze the images with nanometer precision.

The results (Fig. 7) match the theory very well. The tuning range is about 0.05 μ m at 5 V and the resolution is roughly an order of magnitude smaller. The measured frequency response (Fig. 8) has the first mode at 1–2 kHz due to the very compliant flexure. Fig. 9 shows the measured diffraction efficiency over

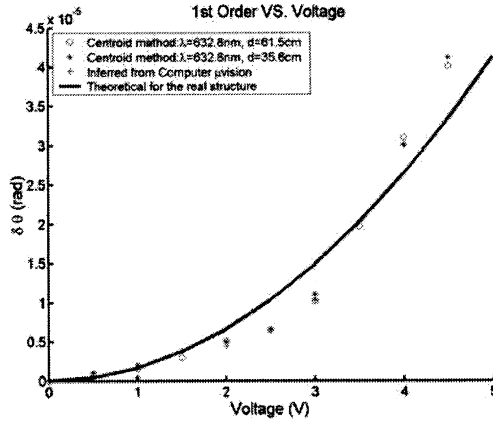


Fig. 7. Diffraction angular change against applied voltage for electrostatic device. The centroid method compares the first-order image centroids before and after actuation.

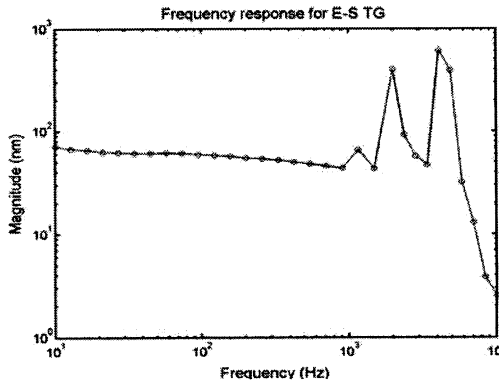


Fig. 8. Frequency response of electrostatic gratings, depicting resonance above operating range.

different actuation voltages. Both device design and fabrication process optimizations are underway.

The piezoelectric-actuated device demonstrated a 68 ± 2 nm membrane deformation in the x -lateral direction at 3.0 V actuation, as shown in Fig. 10. This corresponds to a 0.9 nm period change on a 4 μ m period grating. The gratings also show an expected shrinkage in the y -lateral direction due to deformation in the x -lateral direction. The membrane deformation is in agreement with theory and suggests a d_{31} coefficient of -90 pC/N. The PZT polarization-electric field hysteresis behavior, due to the domain reorientations,

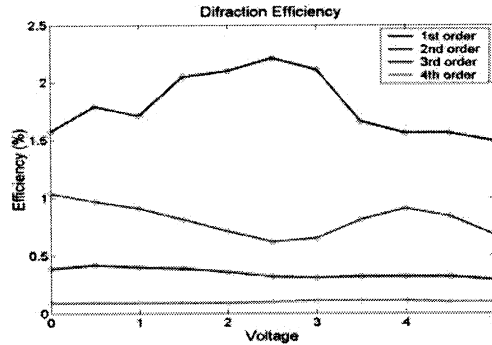


Fig. 9. Diffraction efficiency of electrostatic grating against applied voltage. The efficiency is lower than previously measured values of 12% due to the absence of the reflective metal deposition in this device batch.

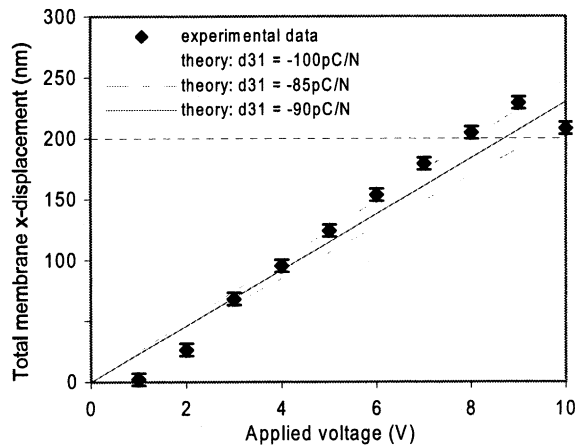


Fig. 10. Piezoelectric membrane deformation versus actuation voltage (measured with computer microvision [6]), in comparison with theory. The noise floor is 2.3 nm.

is evident in the actuation of the membrane, illustrated in Fig. 11 wherein the membrane is actuated from -10 to $+10$ V, and matches with direct hysteresis measurements of the PZT thin-film. First and second order diffraction efficiencies were measured at 7.6% and 5.0% respectively. With the as-measured deformation range, the angular change is estimated at 0.1 mrad at 10 V applied voltage, suggesting a resolution on the order of microradians. Detailed measurements on the resolvable angular change and accurate control of the sub-nanometer deformation are being investigated.

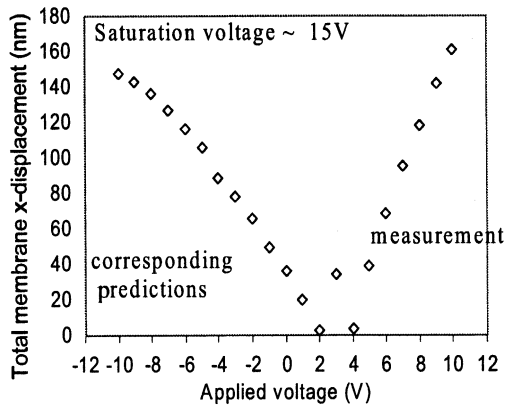


Fig. 11. Deformation pulled with saturation voltage (-15 V) and step-wise increased to 10 V (measured with computer microvision [6]). Results depict domain reorientation in PZT grains.

5. Conclusion

We have designed, fabricated, and tested two novel MEMS analog tunable gratings, with electrostatic and piezoelectric actuators. The extrapolated performance of the electrostatic-actuated device is a wide tunable range of milliradians with resolution of three orders of magnitude smaller at actuation voltage below 30 V. Moreover, the piezoelectric-actuated tunable grating demonstrates a period change on the order of a nanometer, agreeing well with our analytical models, and suggests a resolution on the order of microradians. We have demonstrated the preliminary function of our designs.

Acknowledgements

We are grateful to Kurt Broderick, Salil Desai, Dennis Freeman, Carlos Hidrovo, Gregory Nielson, Martin Schmidt, and Arnab Sinha for their assistance. This project is funded by ASML and the National Science Foundation through the CAREER Award to George Barbastathis.

References

- [1] R.B. Apte et al., Grating light valves for high resolution displays, in: Solid State Sensors and Actuators Workshop, Hilton Head, SC, June 1994, pp. 1–6.
- [2] M.B. Sinclair et al., Synthetic spectra: A tool for correlation spectroscopy, *Applied Optics* 36 (15) (1997) 3342–3348.

- [3] W.C. Tang et al., Lateral driven polysilicon resonant microstructures, in: Proceedings of the IEEE MEMS Workshop, Salt Lake City, Utah, February 1989, pp. 53–59.
- [4] M.S. Weinberg, Working equations for piezoelectric actuators and sensors, *Journal of Microelectromechanical Systems* 8 (4) (1999) 529–533.
- [5] W. Liu et al., Preparation and properties of multiplayer $\text{Pb}(\text{Zr},\text{Ti})\text{O}_3/\text{PbTiO}_3$ thin films for pyroelectric application, *Thin Solid Films* 371 (1–2) (2000) 254–258.
- [6] D.M. Freeman et al., Multidimensional motion analysis of MEMS using computer microvision, in: *Solid State Sensors and Actuators Workshop*, Hilton Head, SC, June 1998, pp. 150–155.